Self-Assembly Hot Paper

International Edition: DOI: 10.1002/anie.201600035
German Edition: DOI: 10.1002/ange.201600035

End-Group-Functionalized Poly(α-olefinates) as Non-Polar Building Blocks: Self-Assembly of Sugar–Polyolefin Hybrid Conjugates

*Tessy S. Thomas, Wonseok Hwang, and Lawrence R. Sita**

Abstract: *Living coordinative chain-transfer polymerization of α-olefins, followed by chemical functionalization of a Zn(polymeryl)$_2$ intermediate, provides entry to end-group functionalized poly(α-olefinates) (x-PAOs) that can serve as a new class of non-polar building block with tailorable occupied volumes. Application of these x-PAOs for the synthesis and self-assembly of sugar-polyolefin hybrid conjugates demonstrate the ability to manipulate the morphology of the ultra-thin film nanostructure through variation in occupied volume of the x-PAO domain.*

The self-assembly of amphiphilic materials comprised of chemically linked polar and non-polar segments gives rise to a variety of nanostructures in solution and the solid state that are instrumental for a wide range of existing and future technological applications.[1] As such, there has long been a corollary interest in the development of new classes of molecular and macromolecular building blocks for amphiphilic systems that are amenable to programmed structural changes as a means by which to exert control over the relative magnitudes of entropic and enthalpic contributions to the self-assembly process and thereby over the final nanostructure that is formed.[2] Within these considerations, one of the most important structural parameters to vary is the relative free volume occupied by the polar and non-polar domains of an amphiphile. For example, in the case of surfactants, entropically favorable aggregation of non-polar tails within a solvent that is compatible with polar head groups produces micellar structures that can adopt a variety of shapes as a function of the surfactant packing parameter, N_s, which is defined by the volume of the non-polar tail, V_c, the cross-sectional area of the polar domain of the assembly, a, and the length of the non-polar chain, L_c, according to $N_s = V_c/aL_c$.[3] On a longer length scale, the chemical tethering of polar and non-polar macromolecular chains produces amphiphilic block copolymers (BCPs) in which the enthalpic (repulsive) interaction between immiscible block domains can now drive microphase separation within the bulk BCP material to generate periodic arrays with feature sizes on the nanometer length scale.[4] Which specific solid-state microphase-separated morphology is preferred for a given BCP (for example, body-centered-cubic (BCC) spheres, hexagonally packed cylinders, a bicontinuous gyroid phase, or alternating lamellae) is then dictated by the magnitude of the Flory–Huggins interaction parameter for the pair of block domains, χ, the relative block domain volume fractions, f, the overall block copolymer degree of polymerization, N, and temperature, T. Finally, giant surfactants are a more recent new class of amphiphile that consist of one or more polymer chains that are tethered to a functionalized nanoparticle or inorganic cluster.[5] The self-assembly and phase behavior of giant surfactants in solution and the solid-state possess characteristic features of both small molecule surfactants and of BCPs, and once again, the volume fraction occupied by the non-polar polymer chain strongly factors into the nature and complexity of the final nanostructure.

While extensive investigations over the past several decades with amphiphilic systems have served to produce a rich structural diversity of precursors to polar domains, choices for end-group functionalized saturated hydrocarbons as building blocks for non-polar segments still remain largely limited to: 1) the ubiquitous family of long-chain fatty alcohols,[6] 2) bio-sourced phytanol,[7] 3) end-group-functionalized polyisobutylene derived from low-temperature living cationic polymerization of isobutylene followed by chemical transformations,[8] and more recently, 4) end-group functionalized polyethylene derived from the coordinative chain group transfer polymerization of ethylene.[9–11] Unfortunately, all four of these classes of non-polar building block suffer from the inability to systematically modify occupied free volume through controlled synthetic manipulation of the steric bulk of pendant side chains, and in the case of the first two, the overall length (that is, molecular weight) of the hydrocarbon main-chain. Furthermore, in the case of long-chain alcohols, close-packed aggregation manifests in the crystallization of the non-polar domains at even relatively short chain lengths, and this physical property serves to limit the range of accessible self-assembled nanostructures.[12] Indeed, for polyethylene-based amphiphilic block copolymers, it is crystallization of the polyethylene block domain that often dominates microphase separation in the solid state.[13] Herein, we now document the utility of living coordinative chain-transfer polymerization (LCCTP) of α-olefins as a means by which to access a highly versatile new class of non-polar building block for amphiphilic materials, which is hereafter referred to as end-group functionalized poly(α-olefinates), or x-PAOs for short.[14–16] We further report the results of a preliminary investigation of the use of x-PAOs for the synthesis and self-assembly of the sugar–polyolefin hybrid conjugates shown in Scheme 1 in which the free volume occupied by the non-polar fragment can be easily manipulated by the choice of the starting α-olefin monomer

[*] T. S. Thomas, W. Hwang, Prof. L. R. Sita
Department of Chemistry and Biochemistry, University of Maryland
College Park, MD 20742 (USA)
E-mail: lsita@umd.edu

Supporting information and the ORCID identification number(s) for the author(s) of this article can be found under http://dx.doi.org/10.1002/anie.201600035.

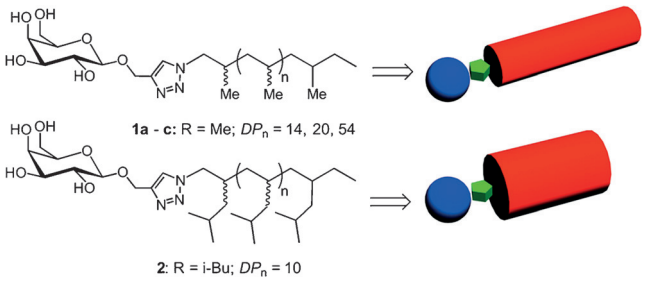

Scheme 1. β-D-galactose-polyolefin hybrid conjugates of narrow polydispersity and varying occupied spatial volumes. In the representations at the right: blue sphere, sugar moiety; green pentagon, triazole linker; red cylinder, polyolefin tail derived from an x-PAO precursor.

(for example, propene or 4-methyl-1-pentene in the case of **1** and **2**, respectively) and by the number average degree of polymerization, DP_n, that can be varied through the LCCTP process that also produces very narrow molecular weight distributions, as characterized by a polydispersity index, $Đ(= M_w/M_n)$ of < 1.15, where M_n and M_w are the number average and weight average molecular weight indices, respectively. In this way, the ramifications of incorporating a "long-thin" vs. a "short-fat" non-polar domain within a targeted amphiphilic material can be easily assessed (compare the top and bottom structures of Scheme 1, respectively). Furthermore, owing to the atactic nature of the polymer stereochemical microstructure afforded by LCCTP that is coupled with pendant side groups along the main chain, the x-PAOs used herein also do not form crystalline domains, even at fairly high molecular weights. This latter feature is attractive for potentially enhancing the ability of amphiphilic nanostructures to sequester lipophilic guests within the non-polar fragments.[1b] Finally, since LCCTP is easily scalable, the availability of kilogram quantities of x-PAOs is realistic.

We have previously reported that the LCCTP of ethene, propene, longer-chain α-olefins, and α,ω-non-conjugated dienes can be achieved using the transition-metal initiator, $[Cp^*Hf(Me)\{N(Et)C(Me)N(Et)\}][B(C_6F_5)_4]$ ($Cp^* = \eta^5$-C_5Me_5), that is generated in situ through activation of the pre-initiator, $[Cp^*Hf\text{-}(Me)_2\{N(Et)C(Me)N(Et)\}]$ (**3**) by a stoichiometric amount of the co-initiator, $[PhNHMe_2][B(C_6F_5)_4]$ (**4**), in the presence of excess equivalents of a main-group-metal alkyl, such as diethylzinc ($ZnEt_2$) (**5**).[14,15] The key feature of LCCTP is that due to rapid and reversible polymeryl group (chain) transfer that occurs between the active transition-metal propagators and the inactive main-group metal alkyl species at a rate, ν_{ct}, that is much greater than the rate of propagation of the growing polymer chain at the transition-metal center, ν_p, both populations of active and inactive metal centers appear to propagate at the same rate. Furthermore, as long as the rate constant for chain transfer, k_{ct}, is far greater than the rate constant for propagation, k_p, all the desired features of a traditional living polymerization can still be achieved, including: 1) a tunable value for DP_n that is proportional to the amount of monomer consumed and inversely proportional to the total concentration of polymeryl chains according to: $DP_n = \{[\text{monomer}]_t - [\text{monomer}]_0\}/\{[M_T\text{–}P_A] + n[M_{MG}\text{–}P_A]\}$, where n is the number of equivalent polymeryl groups associated with the concentration of the inactive main-group-metal sites, $[M_{MG}\text{–}P_A]$ (for example $n = 2$ for $ZnEt_2$), and where $[M_T\text{-}P_A]$ represents the concentration of the active transition-metal sites; and 2) very low polydispersities where $Đ \approx 1 + k_p/k_{ct}$ for a dynamic two-state polymerization.[17] An added benefit is that, at the end of LCCTP, and prior to workup, virtually all of the polymer chains are in the form of a $Zn(polymeryl)_2$ product that has reactive zinc–carbon bonds. Accordingly, it is possible to easily prepare a variety of *x*-PAOs through various chemical transformations.[16] In contrast, previous strategies to prepare end-group functionalized atactic and isotactic polypropene have not provided the same degree of control over molecular weight and all these materials possess broad polydispersities.[18]

Scheme 2 presents a summary of the methods used to prepare the x-PAOs, **6**–**9**, of varying DP_n value in the case of **6** and **8**, as well as the intermediate hydroxyl-protected β-D-galactose polyolefin hybrid conjugates, **11** and **12**, and the

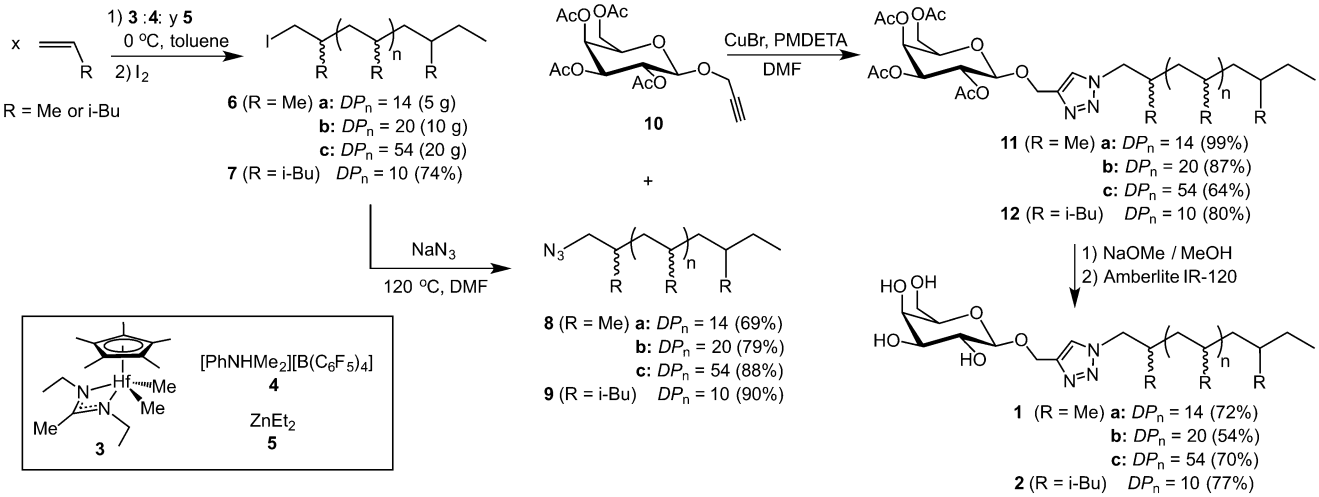

Scheme 2. Summary of synthetic methods employed to prepare x-PAO derivatives and sugar–polyolefin hybrid conjugates.

deprotected derivatives **1** and **2** that were the ultimate targets of the present study. To begin, by simply adjusting the initial ratio of **3** and **4**, relative to **5**, and overall polymerization time, multi-gram quantities of narrow polydispersity *x*-PAOs for a given pendent R group (for example R = Me and i-Bu) were easily obtained that differ only with respect to DP_n values.[19] Furthermore, the conversion of **6** and **7** into the corresponding azido derivatives **8** and **9** proceeded in excellent yields of 70–90% under the conditions employed.[19] To assemble the sugar-polyolefin hybrid conjugates, copper-catalyzed alkyne–azido click coupling of β-D-galactose tetraacetate *O*-propargyl glycoside (**10**)[20] was first conducted with **8** and **9** to produce the respective tetraacetate derivatives, **11** and **12**, respectively, in high yields.[21] Base-mediated removal of the acetate protecting groups was then performed to provide the β-D-galactose-polyolefin hybrid conjugates, **1** and **2**, respectively, that were fully characterized by a suite of analytical methods, including NMR spectroscopy and MALDI-TOF-MS.[19]

The results of an investigation of the self-assembly of the peracetylated derivatives, **11** and **12**, and of the de-acetylated β-D-galactose-polyolefin hybrid conjugates, **1** and **2**, in polar solutions will be presented elsewhere. Herein, we present the results of studies that were focused on the generation and characterization of ultra-thin films (≤100 nm thick) of these materials that are supported on the native silicon oxide layer of Si(100).[19] To begin, spin casting at 2000 rpm of 0.1%–1% (w/v) solutions of **11** and **12** in acetone onto freshly cleaned Si(100) wafers provided ultra-thin films that were analyzed by phase-sensitive, tapping-mode atomic force microscopy (ps-tm AFM).[22] As Figure 1 illustrates, all of the peracetylated derivatives, **11** and **12**, were found to form nanostructured films consisting of stacked bilayer assemblies.[23] Cross-sectional analyses provided an average step-height, *h*, of 4.91 ± 0.05 nm for **11a** (DP_n = 14, $Đ$ = 1.15), 5.32 ± 0.24 nm for **11b** (DP_n = 20, $Đ$ = 1.15), 6.30 ± 0.18 nm for **11c** (DP_n = 54, $Đ$ = 1.04), and 3.69 ± 0.24 nm for **12** (DP_n = 10, $Đ$ = 1.14). In addition to using DP_n to adjust the thickness of each bilayer, control of the number of stacked bilayers within the ultra-thin films could be achieved by simply adjusting the concentration of the acetone solutions used for spin-casting (Figure 1A vs. 1B). The number of stacked bilayers, or total height of the assembly, further appears to be constrained by the contact area that the bilayer film makes with the substrate (Figure 1A). This latter observation raises the possibility that a patterned substrate might be potentially used for the hierarchical directed self-assembly of nanopatterned arrays of stacked bilayers and with control over stacking numbers.[24] Finally, depth-profiling elemental analysis of the stacked bilayer ultra-thin film of **11a–c** by angle-dependent X-ray photoelectron spectroscopy (XPS) strongly supports a head-tail-tail-head (H-T-T-H) bilayer structure in which the sugar head group is preferentially in contact with the native silicon oxide layer of the Si(100) surface. A final H-T monolayer then provides a top-coat on the outermost bilayer structure to present a hydrophobic surface at the air-film interface.[23]

In contrast to the well-defined and stable stacked bilayer assemblies of ultra-thin films of **11** and **12**, similar spin-casting of 0.5–1% (w/v) solutions of **1** in hexane produced rather surprising results. More specifically, as Figure 2A presents, ps-tm-AFM analysis of an "as-cast" ultra-thin film (70–100 nm thick) of **1b** onto the native SiO_2 layer of Si(100) revealed a fingerprint microphase-separated morphology with a domain spacing, *d*, of 6.40 ± 0.19 nm that increased in long-range order upon thermal annealing (60 °C, 14 h; Figure 2B). These observations, along with transmission electron microscopy (TEM) of ultra-thin films of **1b** that were supported on a 15 nm-thick TEM-transparent silicon nitride (Si_2N_3) membrane, and preliminary grazing-incidence small-

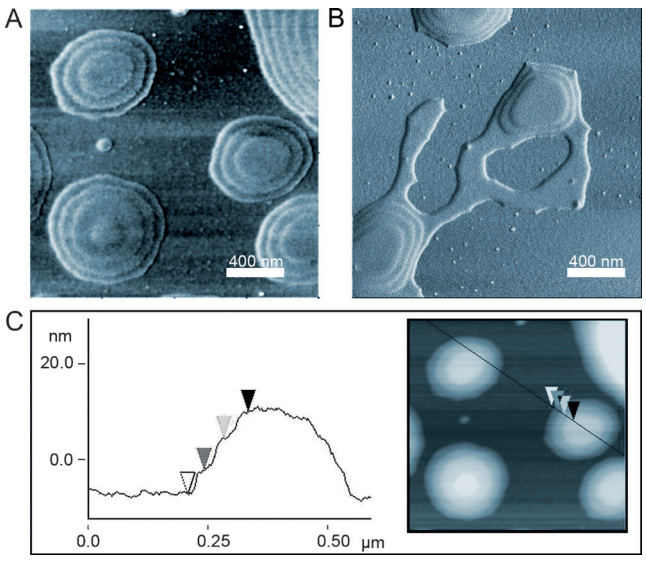

Figure 1. ps-tm-AFM analysis of "as-cast" ultra-thin films of **11c**: A) phase map from 1 wt% (w/v) acetone solution, B) phase map from 0.1% wt (w/v) acetone solution, and C) cross-sectional analysis of height map of sample in (A).

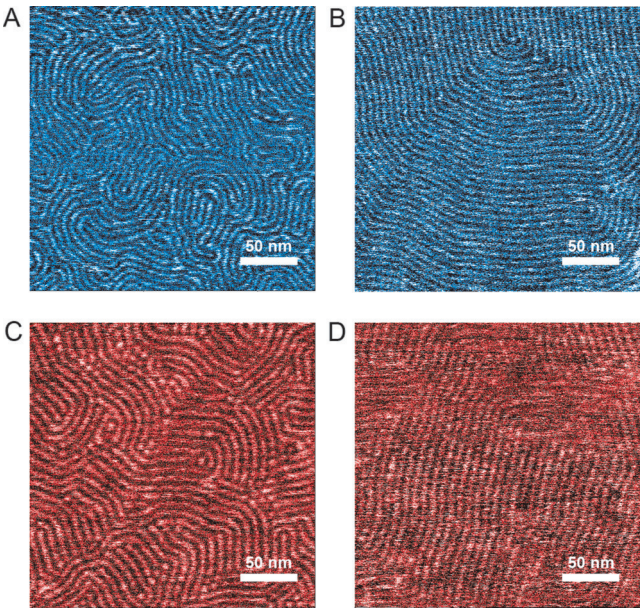

Figure 2. ps-tm-AFM analyses (phase map) of ultra-thin films (70–100 nm thick) of A) unannealed **1b**, B) thermally annealed (60 °C, 14 h) **1b**, C) unannealed **1c**, and D) thermally annealed **1c**.

angle X-ray scattering (GISAXS)[25] support a cylindrical morphology for **1b**.[19,26] Interestingly, ps-tm-AFM analysis of unannealed and annealed ultra-thin films of **1c** once again revealed the existence of a microphase-separated morphology but with a slightly larger d value of 8.14 ± 0.32 nm being obtained (Figures 2C and 2D). It is highly likely that the ability to observe two clearly distinguishable d values for relatively small difference in DP_n values for ultra-thin films of **1** is due to the very small polydispersity values $Đ$ that are associated with the *x*-PAO building blocks used to prepare these materials. However, preliminary GISAXS data obtained for these ultra-thin films of **1c** suggest that a lamellar phase is now likely dominant.[19,26]

The ability to generate nanostructured ultra-thin films of sugar–polyolefin hybrid conjugates with sub-10 nm feature sizes is a current goal for possible applications in nanolithography.[1d–f,27,28] In this regard, since the domain spacing period, d, of a microphase-separated diblock BCP nanostructure scales as $d \approx N^{2/3}\chi^{1/6}$, the value of χ must be very high to maintain segregation strength as the chain length of the diblock copolymer N decreases.[27] In the present work, it was therefore of significant interest to determine if structural changes made to the occupied free volumes of the *x*-PAO building blocks (Scheme 1) could be used to directly modify the nanostructured morphology of the ultra-thin films of sugar–polyolefin hybrid conjugates, and as Figure 3 reveals, this appears to be the case. More specifically, TEM (using Si_2N_3 membranes), ps-tm-AFM and GISAXS analyses of unannealed and thermally annealed (60 °C, 17 h) ultra-thin films of **2** display a strikingly different nanostructured morphology from those of either **1b** and **1c**, with a nominal domain spacing $d = 5.28 \pm 0.51$ nm (Figure 3B).[19] Further experimental and theoretical studies are now required to establish a set of first-principles that might be used to predict the solid-state phase behavior of this novel class of sugar–polyolefin hybrid conjugates that are represented by **1** and **2**.

In summary, the LCCTP of α-olefins, followed by chemical functionalization of the intermediate Zn(polymeryl)$_2$ species, has been shown to be a powerful strategy by which to produce a highly versatile new category of nonpolar building blocks in the form of *x*-PAOs of very narrow polydispersity, tunable DP_n, and tailorable occupied volumes. Along with further investigations of sugar–polyolefin hybrid conjugates, additional efforts are now being directed to expand the utility of these readily available *x*-PAOs as building blocks for new advance materials and applications.

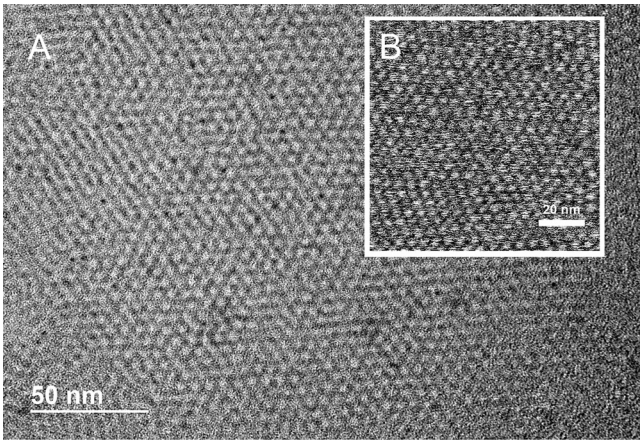

Figure 3. A) TEM image of ultra-thin film (30 nm-thick) of **2** supported on a 15-nm thick Si_2N_3 membrane, B) ps-tm-AFM phase map of a similar ultra-thin film of **2** supported on the native oxide layer of Si(100).

Acknowledgements

Funding for this work was provided by the National Science Foundation (CHE-1152294). We also wish to acknowledge support through a DOE GAANN fellowship to T.S.T. (P200A15003).

Keywords: click chemistry · living polymerization · polyolefins · self-assembly · sugars

How to cite: *Angew. Chem. Int. Ed.* **2016**, *55*, 4683–4687
Angew. Chem. **2016**, *128*, 4761–4765

[1] a) D. Myers, *Surfactant Science and Technology*, *Third Edition*, Wiley, Hoboken, NJ, **2006**; b) V. P. Torchilin, *Adv. Drug Delivery Rev.* **2006**, *58*, 1532–1555 and references cited therein. c) T. T. L. Nguyen, A. Edelen, B. Neighbors, D. A. Sabatini, *J. Colloid Interface Sci.* **2010**, *348*, 498–504; d) I. W. Hamley, *Prog. Polym. Sci.* **2009**, *34*, 1161–1210; e) K. Koo, H. Ahn, S. W. Kim, D. Y. Ryu, T. P. Russell, *Soft Matter* **2013**, *9*, 9059–9071; f) J. D. Cushen, I. Otsuka, C. M. Bates, S. Halila, S. Fort, C. Rochas, J. A. Easley, E. L. Rausch, A. Thio, R. Borsali, C. G. Willson, C. J. Ellison, *ACS Nano* **2012**, *6*, 3424–3433.

[2] a) C. C. Ruiz, *Sugar-Based Surfactants: Fundamentals and Applications*, CRC Press, Boca Raton, FL, **2009**; b) B. Fell in *Anionic Surfactants: Organic Chemistry* (Ed.: H. W. Stache), Marcel Dekker, New York, **1996**; c) G. C. Feast, O. E. Hutt, X. Mulet, C. E. Conn, C. J. Drummond, G. P. Savage, *Chem. Eur. J.* **2014**, *20*, 2783–2792.

[3] a) J. N. Israelachvili, *Intermolecular and Surfaces Forces.* 2nd ed., Academic Press, London, **1992**, pp. 241–258; b) R. Nagarajan, *Langmuir* **2002**, *18*, 31–38.

[4] I. Hamley, *The Physics of Block Copolymers*, Oxford University Press, New York, **1998**.

[5] a) X. Yu, K. Yue, I.-F. Hsieh, Y. Li, X.-H. Dong, C. Liu, Y. Xin, H.-F. Wang, A.-C. Shi, G. R. Newkome, R.-M. Ho, E.-Q. Chen, W.-B. Zhang, S. Z. D. Cheng, *Proc. Natl. Acad. Sci. USA* **2013**, *110*, 10078–10083; b) C.-H. Hsu, X.-H. Dong, Z. Lin, B. Ni, P. Lu, Z. Jiang, D. Tian, A.-C. Shi, E. L. Thomas, S. Z. D. Cheng, *ACS Nano* **2016**, *10*, 919–929.

[6] a) J. D. Cushen, K. Shanmuganathan, D. W. Janes, C. G. Willson, C. J. Ellison, *ACS Macro Lett.* **2014**, *3*, 839–844; b) M. J. Clemente, J. Fitremann, M. Mauzac, J. L. Serrano, L. Oriol, *Langmuir* **2011**, *27*, 15236–15247.

[7] a) C. Fong, D. Wells, I. Krodkiewska, P. G. Hartley, C. J. Drummond, *Chem. Mater.* **2006**, *18*, 594–597; b) C. Fong, D. Wells, I. Krodkiewska, J. Booth, P. G. Hartley, *J. Phys. Chem. B* **2007**, *111*, 1384–1392; c) H. Wang, S. D. Wettig, *Phys. Chem. Chem. Phys.* **2011**, *13*, 637–642.

[8] a) S. Ummadisetty, J. P. Kennedy, *J. Polym. Sci. Part A* **2008**, *46*, 4236–4242; b) D. E. Bergbreiter, P. N. Hamilton, N. M. Koshti, *J. Am. Chem. Soc.* **2007**, *129*, 10666–10667; c) P. Zare, A. Stojanovic, F. Herbst, J. Akbarzadeh, H. Peterlik, W. H. Binder, *Macromolecules* **2012**, *45*, 2074–2084; d) K. Bauri, P. De, P. N. Shah, R. Li, R. Faust, *Macromolecules* **2013**, *46*, 5861–5870;

e) K. Ren, M. Zhang, J. He, Y. Wu, P. Ni, *ACS Appl. Mater. Interfaces* **2015**, *7*, 11263 – 11271.
[9] a) J. F. Pelletier, A. Mortreux, X. Olonde, K. Bujadoux, *Angew. Chem. Int. Ed. Engl.* **1996**, *35*, 1854 – 1856; *Angew. Chem.* **1996**, *108*, 1980 – 1982; b) G. J. P. Britovsek, S. A. Cohen, V. C. Gibson, P. J. Maddox, *Angew. Chem. Int. Ed.* **2002**, *41*, 489 – 491; *Angew. Chem.* **2002**, *114*, 507 – 509.
[10] For reviews of coordinative chain transfer polymerization, see: a) R. Kempe, *Chem. Eur. J.* **2007**, *13*, 2764 – 2773; b) A. Valente, A. Mortreux, M. Visseaux, P. Zinck, *Chem. Rev.* **2013**, *113*, 3836 – 3857.
[11] a) H. Kaneyoshi, Y. Inoue, K. Matyjaszewski, *Macromolecules* **2005**, *38*, 5425 – 5435; b) R. Briquel, R. J. Mazzolini, T. Le Bris, O. Boyron, F. Boisson, F. Delolme, F. D'Agosto, C. Boisson, R. Spitz, *Angew. Chem. Int. Ed.* **2008**, *47*, 9311 – 9313; *Angew. Chem.* **2008**, *120*, 9451 – 9453; c) I. German, F. D'Agosto, C. Boisson, S. Tence-Girault, C. Soulie-Ziakovic, *Macromolecules* **2015**, *48*, 3257 – 3268.
[12] C. Stubenrauch, *Curr. Opin. Colloid Interface Sci.* **2001**, *6*, 160 – 170.
[13] a) L. Sun, Y. Liu, L. Zhu, B. S. Hsiao, C. A. Avila-Orta, *Polymer* **2004**, *45*, 8181 – 8193; b) R. Schulze, M. M. L. Arras, G. L. Destri, M. Gottschaldt, J. Bossert, U. S. Schubert, G. Marletta, K. D. Jandt, T. F. Keller, *Macromolecules* **2012**, *45*, 4740 – 4748.
[14] For a review of LCCTP, see: L. R. Sita, *Angew. Chem. Int. Ed.* **2009**, *48*, 2464 – 2472; *Angew. Chem.* **2009**, *121*, 2500 – 2508.
[15] a) W. Zhang, L. R. Sita, *J. Am. Chem. Soc.* **2008**, *130*, 442 – 443; b) W. Zhang, J. Wei, L. R. Sita, *Macromolecules* **2008**, *41*, 7829 – 7833; c) J. Wei, W. Zhang, L. R. Sita, *Angew. Chem. Int. Ed.* **2010**, *49*, 1768 – 1772; *Angew. Chem.* **2010**, *122*, 1812 – 1816; d) J. Wei, R. Wickham, L. R. Sita, *Angew. Chem. Int. Ed.* **2010**, *49*, 9140 – 9144; *Angew. Chem.* **2010**, *122*, 9326 – 9330; e) J. Wei, W. Hwang, W. Zhang, L. R. Sita, *J. Am. Chem. Soc.* **2013**, *135*, 2132 – 2135.
[16] A preliminary description of the application of LCCTP for the synthesis of end-group-functionalized atactic polypropene has been presented, see: J. Wei, R. Wickham, L. Sita, *Polym. Prepr.* **2010**, *51*, 370 – 371.
[17] A. H. E. Muller, R. Zhuang, D. Yan, G. Litvinenko, *Macromolecules* **1995**, *28*, 4326 – 4333.
[18] a) T. C. Chung, *J. Organomet. Chem.* **2005**, *690*, 6292 – 6299; b) T. Hagiwara, H. Saitoh, A. Tobe, D. Sasaki, S. Yano, T. Sawaguchi, *Macromolecules* **2005**, *38*, 10373 – 10378; c) B. Lin, D. Lawler, G. P. McGovern, C. A. Bradley, C. E. Hobbs, *Tetrahedron Lett.* **2013**, *54*, 970 – 974; d) S. J. Dalsin, M. A. Hillmyer, F. S. Bates, *ACS Macro Lett.* **2014**, *3*, 423 – 427.
[19] Experimental details are provided in the Supporting Information.
[20] S. K. Mamidyala, M. G. Finn, *J. Org. Chem.* **2009**, *74*, 8417.
[21] a) Special Issue: Click Chemistry (Ed.: W. H. Binder), *Polym. Sci. Macromol. Rapid. Commun.* **2008**, *29*, 943 – 1185; b) T. Isono, I. Otsuka, Y. Kondo, S. Halila, S. Fort, C. Rochas, T. Satoh, R. Borsali, T. Kakuchi, *Macromolecules* **2013**, *46*, 1461 – 1469.
[22] a) M. A. van Dijk, R. van den Berg, *Macromolecules* **1995**, *28*, 6773 – 6778; b) P. Leclère, R. Lazzaroni, J. L. Brédas, J. M. Yu, P. Dubois, R. Jerome, *Langmuir* **1996**, *12*, 4317 – 4320.
[23] A. C. Simonsen, L. A. Bagatolli, *Langmuir* **2004**, *20*, 9720 – 9728.
[24] a) E. Kim, C. Shin, H. Ahn, D. Y. Ryu, J. Bang, C. J. Hawker, T. P. Russell, *Soft Matter* **2008**, *4*, 475 – 479; b) K. G. A. Tavakkoli, K. W. Gotrik, A. F. Hannon, A. Alexander-Katz, C. A. Ross, K. K. Berggren, *Science* **2012**, *336*, 1294 – 1298.
[25] a) P. Müller-Buschbaum, *Anal. Bioanal. Chem.* **2003**, *376*, 3 – 10; b) B. Lee, I. Park, J. Yoon, S. Park, J. Kim, K. Kim, T. Chang, M. Ree, *Macromolecules* **2005**, *38*, 4311 – 4323; c) B. Lee, C. T. Lo, S. Seifert, R. E. Winans, *J. Appl. Crystallogr.* **2006**, *39*, 749 – 751.
[26] A detailed investigation of the structural morphology of these ultra-thin films will be published elsewhere.
[27] a) C. Sinturel, F. S. Bates, M. A. Hillmyer, *ACS Macro Lett.* **2015**, *4*, 1044 – 1050; b) W. J. Durand, G. Blachut, M. J. Maher, S. Sirard, S. Tein, M. C. Carlson, Y. Asano, S. X. Zhou, A. P. Lane, C. M. Bates, C. J. Ellison, C. G. Willson, *J. Polym. Sci. Part A* **2015**, *53*, 344 – 352.
[28] a) K. Aissou, I. Otsuka, C. Rochas, S. Fort, S. Halila, R. Borsali, *Langmuir* **2011**, *27*, 4098 – 4103; b) I. Otsuka, T. Isono, C. Rochas, S. Halila, S. Fort, T. Satoh, T. Kakuchi, R. Borsali, *ACS Macro Lett.* **2012**, *1*, 1379 – 1382.

Received: January 3, 2016
Revised: February 8, 2016
Published online: March 9, 2016

